1994 April 07
ONR Contract N00014-91-C-0128

ALCOA TECHNICAL CENTER
100 TECHNICAL DRIVE • ALCOA CENTER, PA 15069-0001

Microstructurally Based Model of Fatigue Initiation and Growth

J. R. Brockenbrough, A. J. Hinkle, P. E. Magnusen and R. J. Bucci
Product Design and Mechanics Division

Creating Value through Technology

MICROSTRUCTURALLY BASED MODEL OF FATIGUE INITIATION AND GROWTH

J. R. Brockenbrough, A. J. Hinkle, P. E. Magnusen, R. J. Bucci
Product Design and Mechanics Division
Alcoa Technical Center, PA 15069-0001

ABSTRACT

A model to calculate fatigue life is developed based on the assumption that fatigue life is entirely composed of crack growth from an initial microstructural inhomogeneity. Specifically, growth is considered to start from either an ellipsoidal void, a cracked particle, or a debonded particle. The capability for predicting fatigue life from material microstructure is based on linear elastic fracture mechanics principles, the sizes of the crack-initiating microstructural inhomogeneities, and an initiation parameter that is proportional to the cyclic plastic zone size. A key aspect of this modeling approach is that it is linked with a general purpose probability program to analyze the effect of the distribution of controlling microstructural features within the material. This enables prediction of fatigue stress versus life curves for various specimen geometries using distributional statistics obtained from characterizations of the microstructure. Results are compared to experimental fatigue data from an aluminum alloy.

INTRODUCTION

Classically, the fatigue life of a metallic specimen or structure has been thought of in three stages; crack initiation, crack growth and final fracture. As crack measurement techniques have improved and researchers have examined small crack growth, microcracks have been discovered which grow from very early in a structures life. This period of small crack growth can be 50 to 90% of the fatigue life. This suggests that fatigue life can be considered as a two stage process of growth and fracture. Due to the length of time that a structure spends in this early phase of fatigue crack growth it is important to accurately model this behavior.

In metallic structures there is generally a hierarchy of features which can control fatigue. Various researchers have identified some of these features. In 2024-T4 and 7075-T6, Erhardt et. al. [1], indicate cracks started at surface inclusions; Wang [2] in a study of 2024-T3

identified inclusions and tool marks as key initiators; Lukasak and Koss [3] in a study of a particle reinforced MMC identified two failure modes associated with the reinforcing particle; Lankford and Kusenburger [4] linked high strength steel crack initiation to cavitation caused by particle debonding, ; Goto, et. al. [5] identified particles and surface scratches as fatigue initiators in heat-treated 0.45% C steel; Fischmeister, et. al. [6] determined pores and particles to be the initiation sites of a Ni superalloy; Magnusen, et. al. [7] indicated that in 7050-T7451 pores and particles act as initiators. Fracture mechanics and damage tolerant methodologies have been shown to work well for rogue inspectable flaws on the order of 0.01-0.05 inches. The motivating force behind this work is to model the role of alloy microstructure on fatigue durability as identified by cracking that originates from a feature of the microstructure approximately 0.0005-0.01 inches in diameter. The crack is then grown to an inspectable dimension of economic consequence (i.e., a crack requiring diagnostic or corrective action during the operational life of a part).

The principal types of microstructural features of concern are micropores and constituent particles. These microstructural inhomogeneities act as sites for the initiation of fatigue cracks. The next section discusses the basic fracture mechanics approach used to model early fatigue growth. Following sections then discuss the infinite life stress sensitivity and sensitivities of the model to material parameters. Finally, life predictions using the model are compared to experimental lives on an aluminum alloy.

MICROSTRUCTURAL BASED FATIGUE MODELING

The method used for the fatigue life analysis is based on the assumption that fatigue life is entirely composed of crack growth from an initial inhomogeneity [8]. Specifically, growth is considered to start from either an ellipsoidal void, a cracked particle, or a debonded particle. It is assumed that each type of inhomogeneity contains a pseudo crack of equatorial length b. As shown in Figure 1, the particle or void height is h and its width is 2R. The remote stress, σ, is applied in the z direction, perpendicular to the plane of crack growth. It is assumed that for a given far-field cyclic stress, $\Delta\sigma$, the pseudo crack forms in the first few cycles. The pseudo crack can be considered a perturbation of the surrounding stress field for the purpose of calculating the available energy for crack extension in the vicinity of a local pore/particle stress concentration. The length of this pseudo crack is assumed to be proportional to the cyclic plastic zone size ahead of the crack as illustrated in Figure 1. To make these ideas more precise, consider the Trantina-Barishpolsky effective stress intensity factor [9], for the flaw geometry

shown. The stress intensity factor associated with the crack surrounding the inhomogeneity can be expressed as,

$$K_{T-B} = \beta\sigma\sqrt{\pi b} \tag{1}$$

where the dimensionless term β addresses the local microfeature and is given by,

$$\beta = \frac{2}{\pi} + B\left(1.12k_t - \frac{2}{\pi} - 1\right)\left(\frac{R}{b+R}\right)^{10} + \left(\frac{R}{b+R}\right)^{1.8} \tag{2}$$

Here B is a constant that has the value 1 for a void, 2 for a bonded cracked particle, and 0.3 for an debonded particle. k_t is the local elastic stress concentration factor for the ellipsoidal void or particle without the crack. Note that β depends on the geometry through the ratio R/(b+R), so that for b >> R, Equations 1 and 2 reduce to the stress intensity factor solution for an embedded elliptical crack, where the void or particle lacks influence on the stress intensity factor. At the other extreme, for b = 0, from Equation 1, the stress intensity factor is zero. Under the imposition of a far-field cyclic stress range $\Delta\sigma$, the cyclic stress intensity factor is,

$$\Delta K_{T-B} = \beta\Delta\sigma\sqrt{\pi b} \tag{3}$$

An estimate of the cyclic plastic zone size associated with ΔK_{T-B} is, [10]

$$r^* = \frac{1}{\pi}\left(\frac{\Delta K_{T-B}}{2\sigma_y}\right)^2 \tag{4}$$

where σ_y is the yield strength of the material. The procedure used to calculate the parameter, b, is to equate it to this measure of plastic zone size. Thus, solve Equation 3 for b and equate it to the plastic zone size of Equation 4. This amounts to finding the ratio R/(b+R) that satisfies

$$\frac{\beta\Delta\sigma}{2\sigma_y} = 1 \tag{5}$$

THRESHOLD STRESS FOR INHOMOGENEITY INITIATED FATIGUE

Equation 5 can be used directly to estimate the fatigue threshold stress, or the stress which yields infinite life, $\Delta\sigma_\infty$. For infinite life, b = 0, and

$$\Delta\sigma_\infty = \frac{2\sigma_y}{\frac{2}{\pi} + B\left(1.12k_t - \frac{2}{\pi} - 1\right) + 1} \tag{6}$$

Although the number of cycles to failure is sensitive to the initial void or particle size, Equation 6 suggests that if fatigue life is controlled by the growth of a crack from an inhomogeneity, then the infinite life stress is independent of void or particle size. It is proportional to yield strength and shows a strong dependence on local stress concentration factor, k_t, and the type of inhomogeneity through B. For voids, B = 1 and Equation 6 becomes,

$$\Delta\sigma_{\infty-\text{voids}} = \frac{2\sigma_y}{1.12k_t} \tag{7}$$

For cracked particles, B = 2 and Equation 6 becomes,

$$\Delta\sigma_{\infty-\text{particles}} = \frac{2\sigma_y}{2.24k_t - 1 - \frac{2}{\pi}} \tag{8}$$

A plot of the sensitivity of the infinite life stress to the local stress concentration factor is shown in Figure 2 for both voids and cracked particles. Figure 2 shows that voids affect the infinite life stress more severely than uncracked particles. For voids, a lower limit on the stress concentration factor is a smooth sphere for which k_t is about 2. At this point the ratio of infinite life stress to yield stress is about 0.9. For Equations 7 and 8 it is assumed that the yield strength is an upper limit on the infinite life stress for the mechanism of fatigue crack growth from a void or particle. This assumption sets limits on the stress concentration factors below which little improvement in infinite life stress is expected. For voids, improvements are possible up to the point at which the void is the shape of a smooth sphere which is the minimum stress concentration possible. For non-spheres there is a dramatic drop in the infinite life stress for small increases in the local stress concentration. For a stress concentration of 3, the ratio of infinite life stress to yield strength has dropped to about 0.6. This corresponds to a circular cavity of elliptical cross-section with aspect ratio 2.5, as depicted in Figure 3. For

particles, the value of stress concentration factor at which the infinite life stress begins to decrease is 1.62. The stress concentration of the particle depends both on particle shape and particle elastic modulus. For a bonded uncracked particle, stress concentrations in the matrix are typically less than 2 [11]. A plot of the stress concentration factor for an isolated rigid elliptical cylindrical particle is shown in Figure 4. For far-field uniform tension, the stress concentration factor for tangential tension is less than 2 for aspect ratios ranging up to 30. This suggests that particle cracking will typically be required before particles can control the infinite life stress. In previous studies on the effects of cracked particles [12,13], it has been shown that cracked particles behave like high aspect ratio voids. This is expected to severely limit the infinite life stress, as shown in Figure 2.

Since the stress concentration factor, k_t, is taken to be a local value at the point where a crack starts to grow, Equation 6 shows that the infinite life stress is sensitive to the smoothness of the void or particle.

SENSITIVITY OF FATIGUE LIFE CURVE TO MODEL PARAMETERS

Crack growth emanating from a metallurgical inhomogeneity is assumed to follow a power law,

$$\frac{da}{dN} = A\Delta K^m \tag{9}$$

where $\frac{da}{dN}$ is the crack growth rate, ΔK is the cyclic stress intensity, and A and m are material constants. For the aluminum plate used in this study, the coefficients obtained by fitting the equation to long crack growth data were, $A = 3.9X10^{-9}$, $m = 4.18$ for an R-ratio of 0.1. ΔK is in units of ksi $\sqrt{in}$.

The sensitivity of the fatigue model to changing material and microstructural parameters can be assessed by calculating the cyclic stress versus life (S/N) curves for the varying material conditions. Specimen failure occurs when $K_{max} = K_{1c}$, a value of $K_{1c} = 25$ ksi $\sqrt{in}$ was used. The influence of particle size on fatigue life is shown in Figure 5 for particle sizes ranging from 0.001 in. to 0.01 in. at a stress concentration value of 2. The yield strength was fixed at 70 ksi. The effect of increasing particle size is to decrease life throughout the range of stress levels. The infinite life stress, however, is insensitive to particle size. Similar trends hold for increasing

void size at constant aspect ratio. The sensitivity of fatigue life to yield strength is shown in Figure 6. Here the particle size is fixed at 0.005 in. and the yield strength is varied from 60 ksi to 80 ksi. As seen, there is almost no change in fatigue life with stress level above the infinite life stress, $\Delta\sigma_{\infty}$. The effect of yield strength on $\Delta\sigma_{\infty}$ is strong; for this mechanism, increasing yield strength increases the threshold stress for fatigue. The results shown in Figures 5 and 6 show that if simultaneously particle (void) size is decreased while increasing yield strength, fatigue lifes are expected to increase at all stress levels. The inhomogeneity aspect ratio or stress concentration has a similar effect on the fatigue life curve as yield stress does. Figure 7 shows a comparison of fatigue S/N curves for particles and voids at different shapes for a yield strength of 70 ksi. The particle or void size is fixed at 0.005 in. It is seen that increasing the stress concentration has a large effect on decreasing the infinite life stress.

COMPARISON OF MODEL CALCULATIONS TO TEST DATA

Open hole fatigue tests were performed to quantify the influence of the various microstructural features on fatigue performance of a high strength aluminum alloy. The fracture surface from the failed specimens were then examined in a scanning electron microscope and the size, location and type of crack initiating inhomogeneity were recorded. Failures in material A were controlled by microporosity, while the failures for material B were generally controlled by cracked particles located at or near the corners of the bore hole. Despite the change in initiation mechanism from material A, where micropores dominated, open hole lifetimes of the two materials are similar.

The model described in the previous sections has been used to calculate open hole fatigue performance of these materials. These calculations have been made using data obtained from the failed fatigue specimen fracture surfaces. Additional input for the calculation included the yield strength, crack growth properties of the material and the local stress concentration factor at the microstructural feature. The local stress concentration factor was determined empirically from fitting the model with the infinite fatigue life data for each material variant. The values obtained for the local stress concentration factor for material A and B are 7.5 and 4.25, respectively. These values can be interpreted to say that the local stress concentration factor became less severe as the microstructural feature has changed. The growth model was linked to the program PROBAN [14] to permit use of statistical information on particle and pore distributions. PROBAN is a general purpose probability analysis program which can be linked to user-defined subroutines to predict crack growth.

The calculated stress versus life curves for each material variant, along with the open hole fatigue test data are shown in Figures 8 and 9. The model was used to calculate the 5%, 50%, and 95% fractiles for each material. (The curves shown are not smooth because only a limited number of stress levels have been analyzed with the model.) In general, the results of the model are in good agreement with the test data. Additional refinement of the model is expected to yield improvement in the ability to predict fatigue behavior of the material variants.

CONCLUSIONS

- Fracture mechanics principles can be applied to microstructural features (0.0005-0.01 inch) that govern fatigue life for both smooth axial and open hole specimen geometries.
- The effects of the initial inhomogeneity size, shape, and location distributions on specimen fatigue life distributions can be analytically predicted.
- Calculations of specimen fatigue S/N curves agree well with actual test data.
- Typically cracked particles are required before particles will control the infinite life stress.
- A particle's or pore's local stress concentration factor is important. The infinite life stress is a maximum when the local stress concentration factor is small.

FUTURE WORK

A goal of modeling is to predict material performance based solely on characterization of the microstructure rather than a postmortem analysis of fatigue failures. Therefore, it is necessary to take metallographic characterizations of the microstructure obtained on random planes and scale the distributions of controlling features to obtain the extreme distributions that are observed through fractography. Extreme value statistics will be used to establish the relationship between the random plane characterizations and the extreme value distributions of constituent particles or voids. Future work will develop capability to predict material fatigue performance based on material microstructure.

ACKNOWLEDGMENTS

The authors wish to acknowledge H. J. Konish, S. M. Miyasato, and R. L. Rolf for many technical discussions and suggestions throughout the course of this work. The authors wish to thank Dr. A. K. Vasudevan and the Office of Naval Research.

REFERENCES

1. Erhart, K. and Grant, N. J., "Behavior of 2024 Aluminum in Low Cycle Fatigue at Low Strain Rates as a Function of Temperature," Fracture 1969, Proceeding of the 2nd International Conference, April 13-18, 1969.

2. Wang, D. Y., "An Investigation of Initial Fatigue Quality," *Design of Fatigue and Fracture Resistant Structures, ASTM STP 761*, P. R. Abelkis and C. M. Hudson, Eds., American Society for Testing and Materials, 1982, pp. 191-211.

3. Lukasak, D. A. and Koss, D. A., "Microstructural Influences on Fatigue Crack Initiation in a Model Particulate-reinforced Aluminum Alloy MMC," *Composites*, Volume 24, Number 3, 1993, pp. 262-269.

4. Lankford, J. and Kusenberger, F. N., "Initiation of Fatigue Cracks in 4340 Steel," Metallurgical Transaction, Volume 4, Number 2, 1973, pp. 553-559.

5. Goto, M., Yanagawa, Y., and Nisitani, H., "Statistical Property in the Initiation and Propagation of Microcracks of a Heat-Treated 0.45% C Steel," *JSME International Journal*, Series I, Volume 33, Number 2, 1990, pp. 235-241.

6. Fischmeister, H., Quadfasel, U., Banhardt, V., Bruckner-Foit, A., Jackels, H., Eblinger, P. and Konig, G., "Towards a Probabilistic Lifetime Prediction Model for Aircraft Engine Disks," Translated from *Zeitschrift fur Metallkunde*, Volume 81, October 1990, pp. 707-714.

7. Magnusen, P. E., Hinkle, A. J., Rolf, R. L., Bucci, R. J., and Lukasak, D. A., "Methodology for the Assessment of Material Quality Effects on Airframe Fatigue Durability," Presented at Fatigue 90, Honolulu, HA, July 15-20.

8. A. J. Hinkle, A. F. Grandt, and L. E. Forsythe, "Predicting the Influence of Initial Material Quality on Fatigue Life," Presented at ICAF 93, Stockholm, Sweden, June 07-11, 1993.

9. G. G. Trantina and M. Barishpolsky, "Elastic-Plastic Analysis of Small Defects - Voids and Inclusions," *Engineering Fracture Mechanics*, Vol. 20, No. 1, 1984, pp. 1-10.

10. S. Suresh, Fatigue of Materials, Cambridge University Press, 1991.

11. R. E. Peterson, Stress Concentration Factors, John Wiley, 1974.

12. W. H. Hunt, Jr., J. R. Brockenbrough, P. E. Magnusen, "An Al-Si-Mg Composite Model System: Microstructural Effects on Deformation and Damage Evolution," Scripta Metallurgica Et Materialia, Vol. 25, p. 15, 1991.

13. J. R. Brockenbrough, F. Zok, "On the Role of Particle Cracking in Flow and Fracture of Metal Matrix Composites," Alcoa Report # 57-14-93, 1993.

14. Det norske Veritas, PROBAN: General Purpose Probabilistic Analysis Program, Veritas Sesam Systems, Hovik, Norway, January 1992.

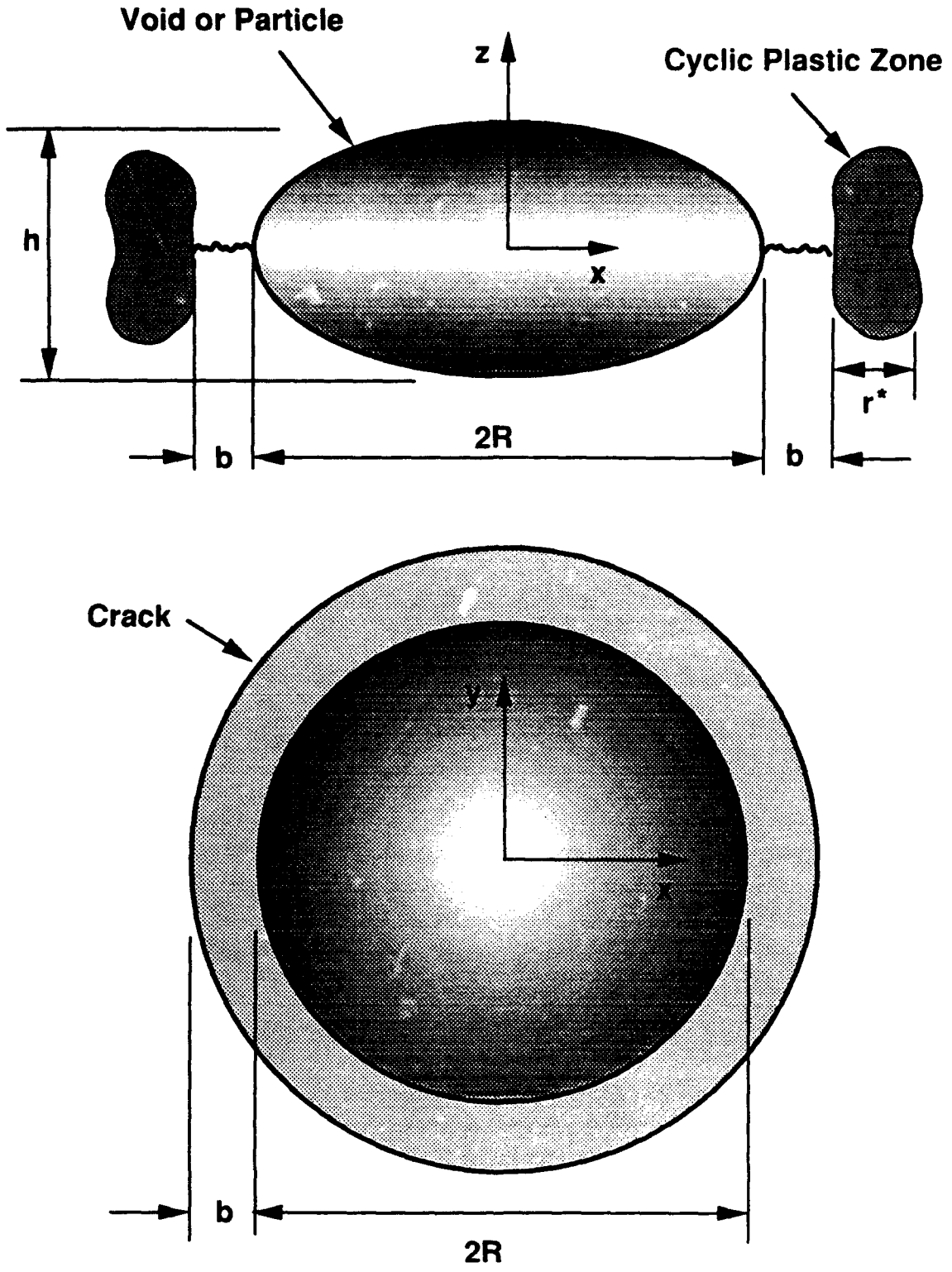

Figure 1. Model for the initial crack size from an ellipsoidal inhomogeneity.

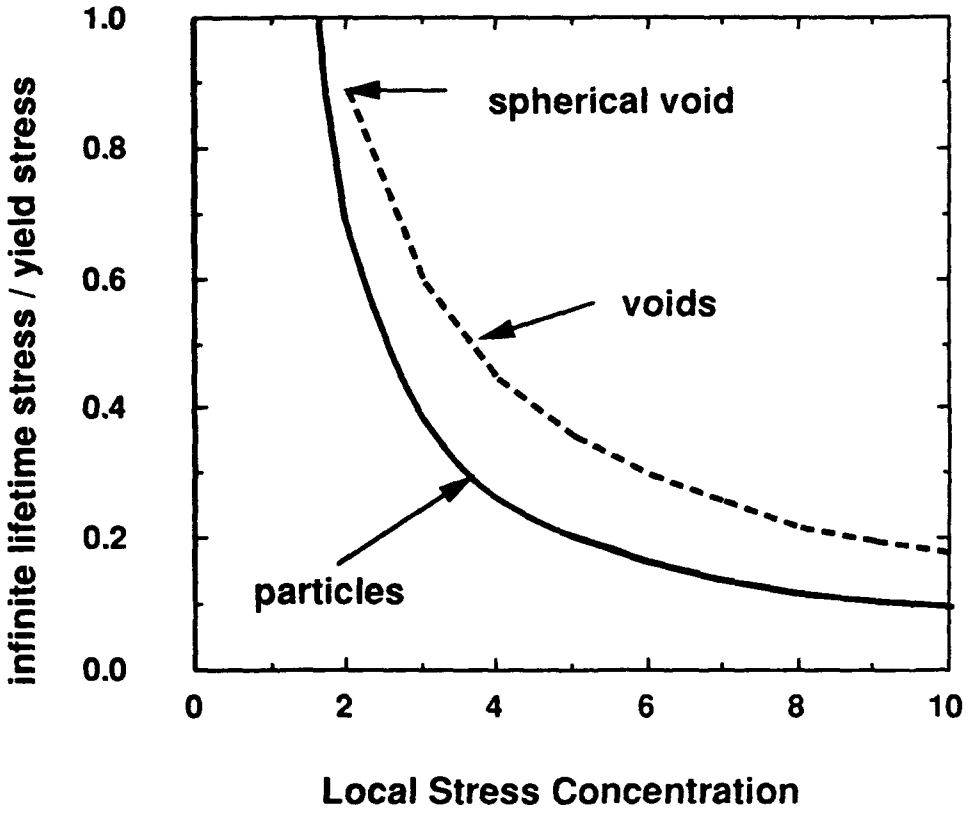

Figure 2. Sensitivity of Threshold Stress to Stress Concentration.

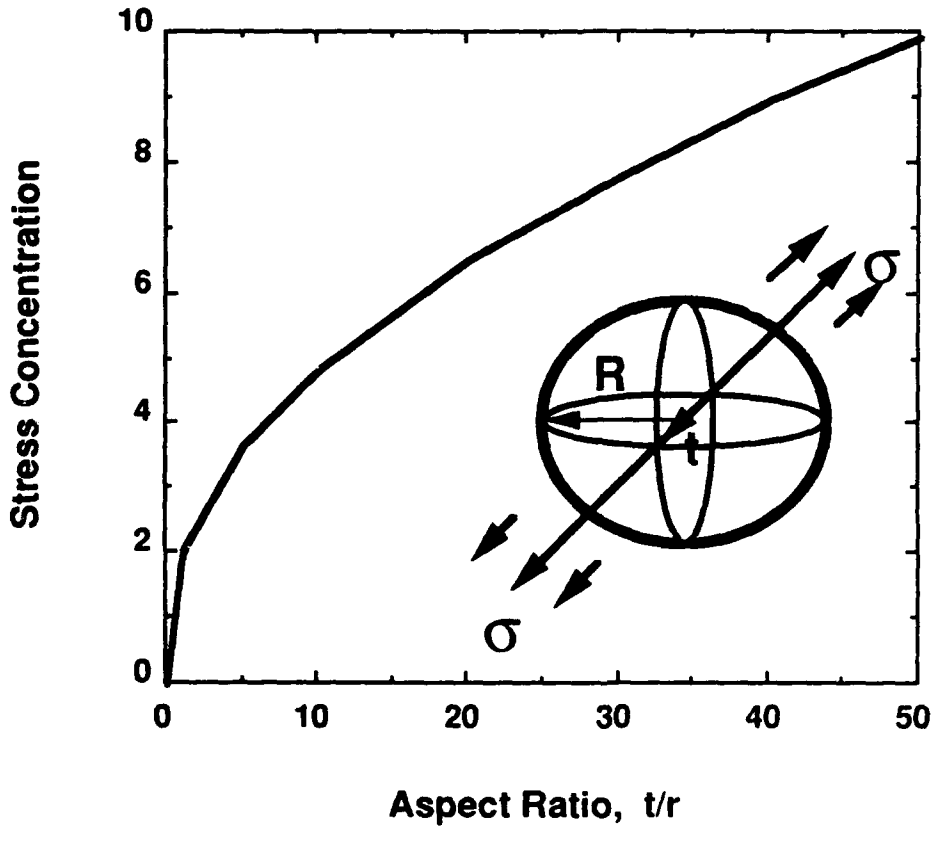

Figure 3. Stress Concentration for a circular cavity of elliptical cross-section.

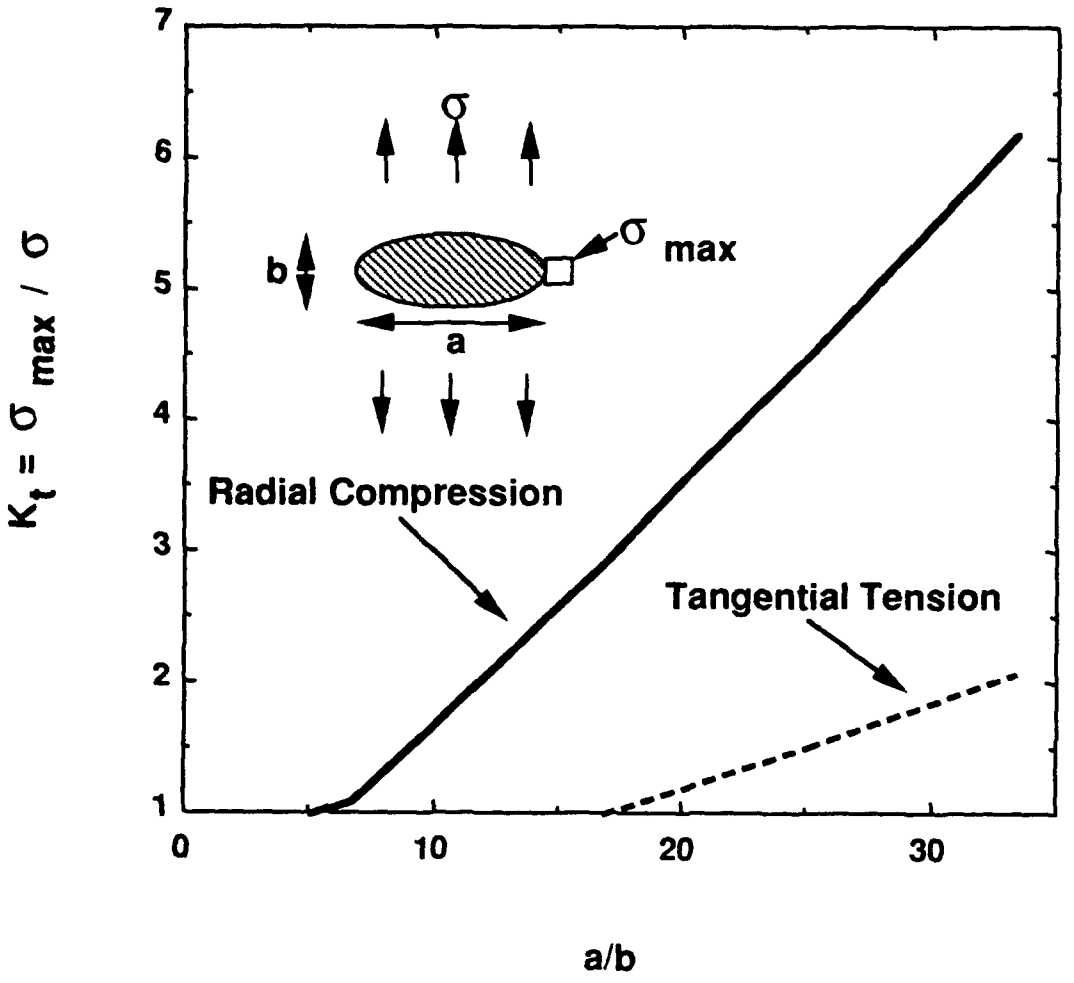

Figure 4. Stress Concentration Factors for Isolated Rigid, Elliptical, Cylindrical Inclusion

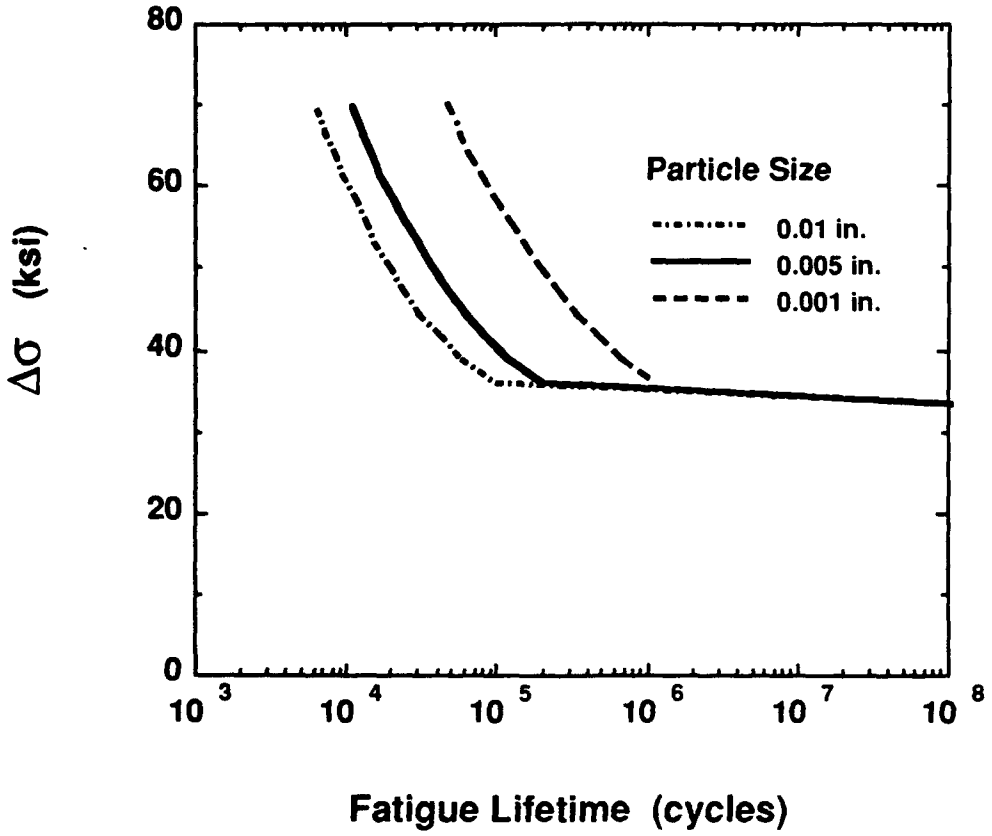

Figure 5. Sensitivity of fatigue lifetime curve to particle size for yield strength of 70 ksi.

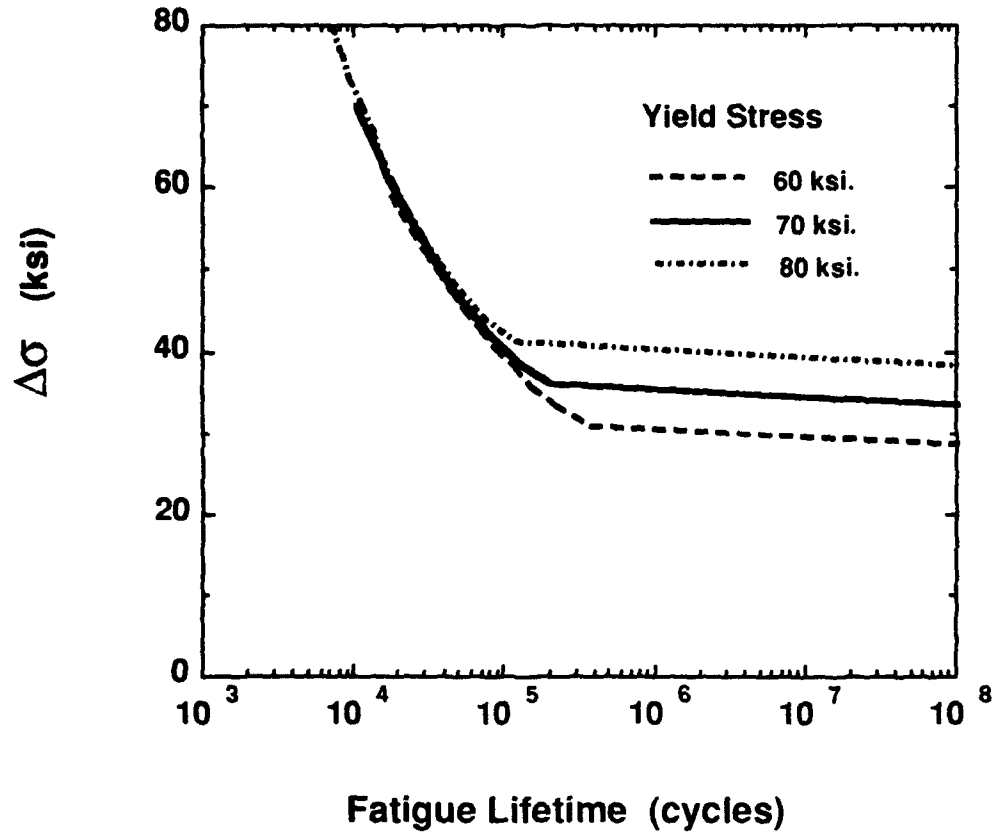

Figure 6. Sensitivity of fatigue lifetime curve to yield stress for particle size of 0.005 in., k = 2

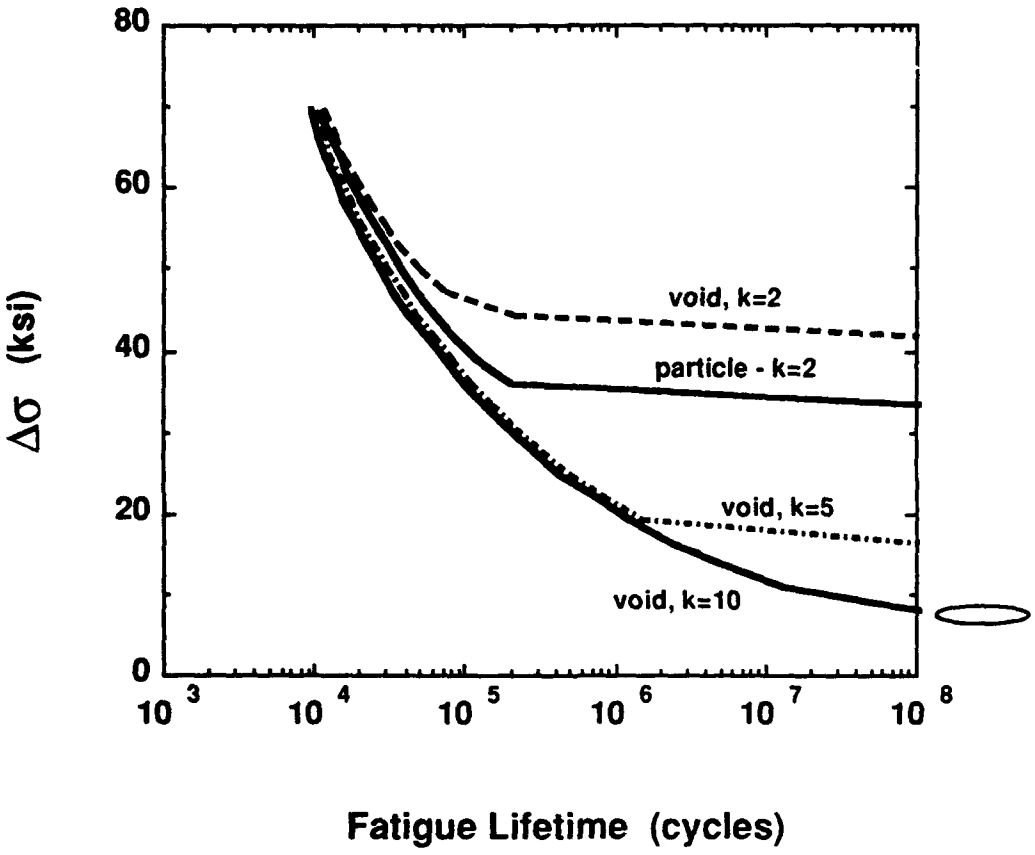

Figure 7. Comparison of fatigue lifetime curves for particles and voids at different particle shapes for yield strength 70 ksi., particle size = 0.005 in.

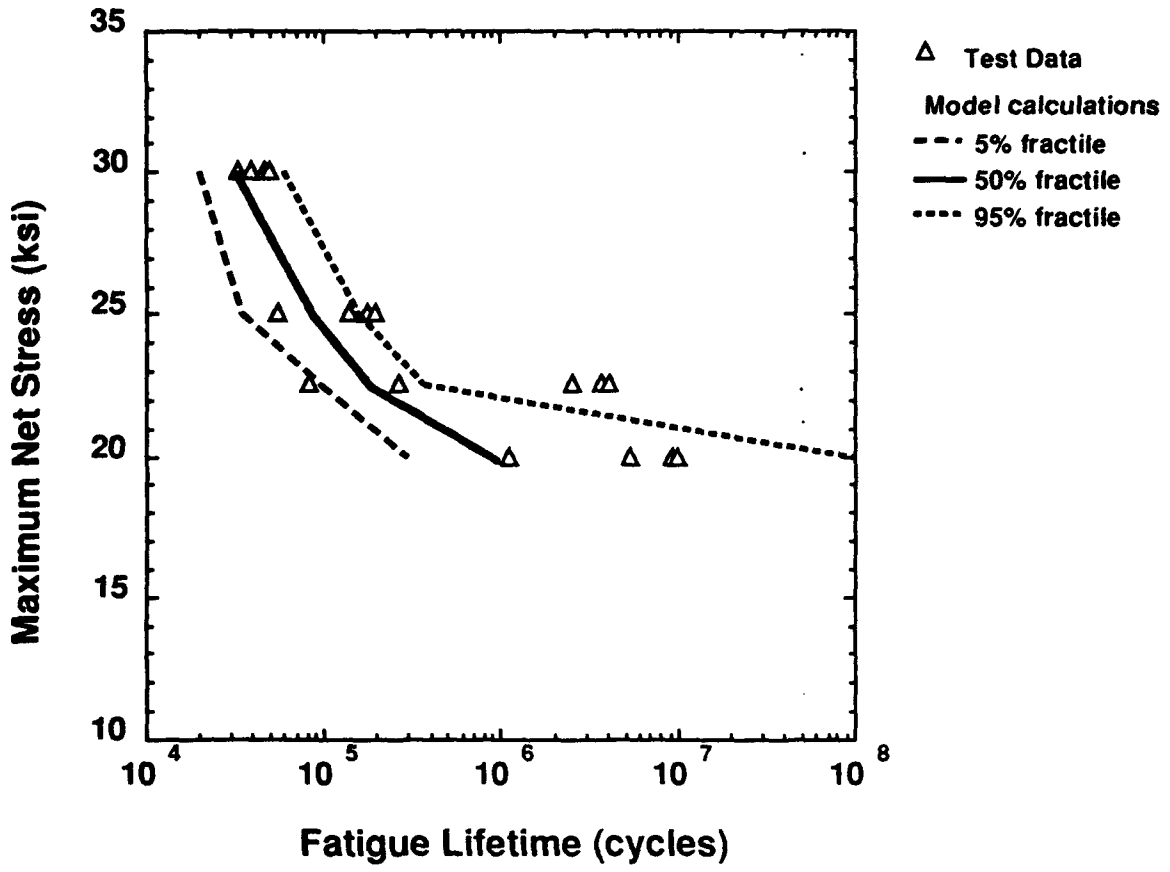

Figure 8. Calculated stress versus life curves for Material A along with the open hole fatigue test data. Tests conducted at R=0.1, LT orientation, freq.=30 Hz, lab air.

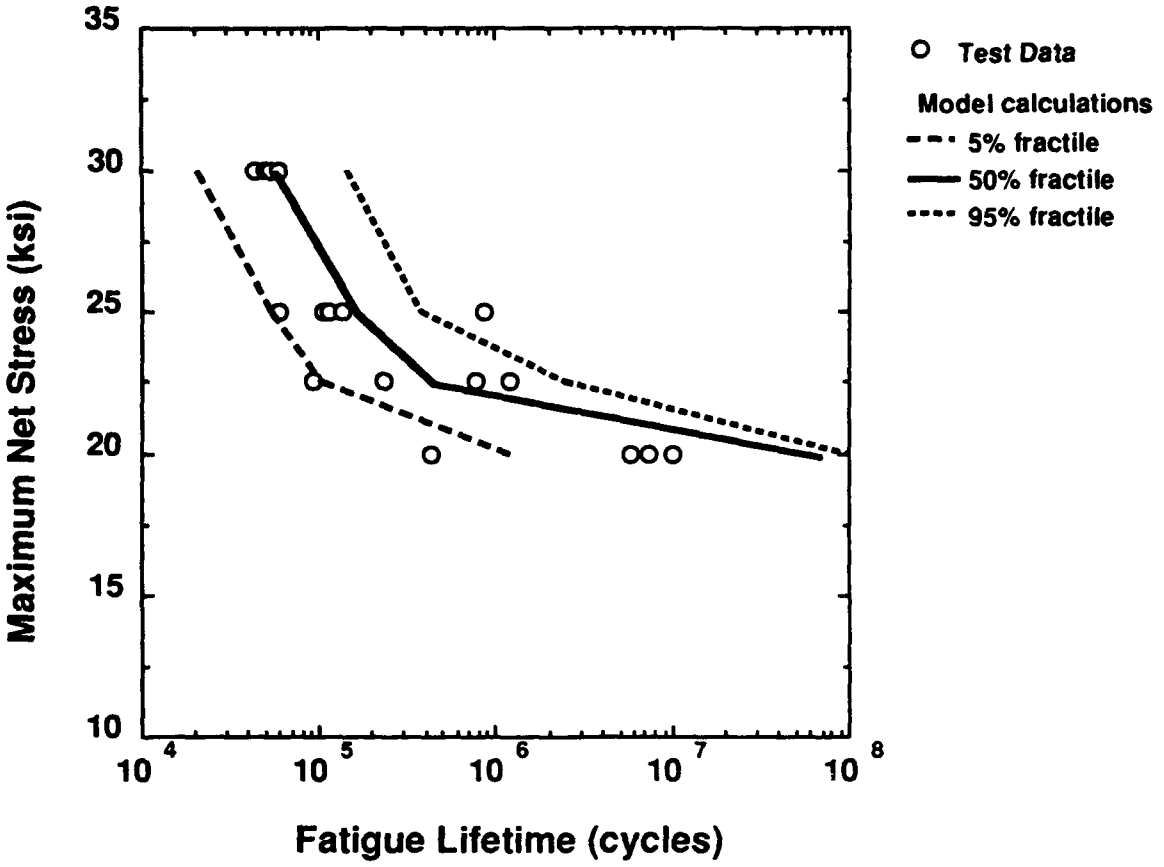

Figure 9. Calculated stress versus life curves for Material B along with the open hole fatigue test data. Tests conducted at R=0.1, LT orientation, freq.=30 Hz, lab air.